Published in final edited form as:

Am J Transplant. 2018 April ; 18(4): 855–867. doi:10.1111/ajt.14567.

Anti-CD47 Monoclonal Antibody Therapy Reduces Ischemia-Reperfusion Injury of Renal Allografts in a Porcine Model of Donation after Cardiac Death

Min Xu[1,†], **Xuanchuan Wang**[1,†], **Babak Banan**[1], **Danielle L. Chirumbole**[1], **Sandra Garcia-Aroz**[1], **Aparna Balakrishnan**[1], **Deepak K. Nayak**[1], **Zhengyan Zhang**[1], **Jianluo Jia**[1], **Gundumi A. Upadhya**[1], **Joseph P. Gaut**[2], **Ronald Hiebsch**[3], **Pamela T. Manning**[3], **Ningying Wu**[4], **Yiing Lin**[1,╪], and **William C. Chapman**[1,╪]

[1]Department of Surgery, Section of Abdominal Transplantation, Washington University School of Medicine, St. Louis, MO

[2]Department of Pathology and Immunology, Washington University School of Medicine, St. Louis, MO

[3]Tioma Therapeutics, Inc, St. Louis, MO

[4]Department of Surgery, Division of Public Health Sciences, Washington University School of Medicine, St. Louis, MO

Abstract

We investigated whether blockade of the CD47 signaling pathway could reduce ischemia-reperfusion injury (IRI) of renal allografts donated after cardiac death (DCD) in a porcine animal model of transplantation. Renal allografts were subjected to 30 min of warm ischemia, 3.5 hours of cold ischemia and then perfused with a humanized anti-CD47 monoclonal antibody (CD47mAb) in the treatment group or HTK solution in the control group (n=4/group). The animals were euthanized 5 days after transplantation. At the time of reperfusion, indocyanine green-based *in vivo* imaging showed that CD47mAb-treated organs had greater and more uniform reperfusion. On post-transplant days 3–5, the treatment group had lower values compared to the control for creatinine and blood urea nitrogen. Histological examination of allograft tissues showed a significant decrease of acute tubular injury in the CD47mAb-treated group compared to control. Compared to the control group, CD47mAb treatment significantly decreased genes expression related to oxidative stress (*sod-1*, *gpx-1*, and *txn*), the inflammatory response (*il-2*, *il-6*, *inf-g* and *tgf-b*), as well as reduced protein levels of BAX, Caspase-3, MMP2, and MMP9. These

╪Correspondence to: William C. Chapman, chapmanwi@wudosis.wustl.edu; or Yiing Lin, liny@wudosis.wustl.edu.
†These authors contributed equally to this work.
DR YIING LIN (Orcid ID : 0000-0002-0317-7608)

Disclosure

The authors of this manuscript have conflicts of interest to disclose as described by the American Journal of Transplantation. William C. Chapman is a founder of Pathfinder Therapeutics (no equity interests) and an advisory board of Novartis Pharmaceutical. Ronald Hiebsch and Pamela T. Manning are employees and stockholders of Tioma Therapeutics, Inc. The other authors have no conflicts of interest to disclose.

Supporting Information

Additional Supporting Information may be found in the online version of this article.

data demonstrate that CD47mAb blockade decreases IRI and subsequent tissue injury in DCD renal allografts in a large animal transplant model.

Introduction

Kidney transplantation after dialysis has been shown to improve survival in patients with end-stage renal disease (ESRD) compared to long-term dialysis alone (1). Between 1996 and 2013, the number of reported cases of ESRD in the United States more than doubled, increasing the number of candidates eligible for a kidney transplant (2, 3). Despite this increase in kidney disease, the number of kidney transplants per 100 active wait-list years has decreased over the past decade and the total number of candidates on the waitlist at the end of each successive year has increased (4). These trends highlight the significant challenges that donor shortage poses to kidney transplantation. There are currently nearly 100,000 patients waiting for a kidney transplant in the United States (5).

Due to the growth of the wait-list, transplant centers have begun to consider, in addition to standard criteria donors (SCD), the use of kidneys from unconventional or high-risk donors, such as those with diabetes, hypertension, or acute kidney injury, as well as kidneys obtained through donation after cardiac death (DCD). Several studies have investigated the effects of utilizing these unconventional donor kidneys on outcomes and survival of patients with ESRD. There is some evidence suggesting that kidneys from most types of unconventional donors do provide a survival benefit. However, only DCD transplantation has become prevalent nationally in recent years (6, 7). In the United States, the rate of DCD kidney transplant rose from 3.2% of all deceased donor transplants in 2002 to 17.1% of all deceased donor transplants in 2014 (3, 8).

While utilization of DCD kidneys may expand the pool of available donor organs, one disadvantage is the associated risk of delayed graft function (DGF) (9). DGF is most commonly defined as the need to resume or begin dialysis within seven days of transplant. A significant contributor to the increased risk of DGF after DCD kidney transplant compared to donation after brain death (DBD) kidney transplant is the duration of warm ischemia time (WIT), the time between asystole and the initiation of cold perfusion (10, 11). While all donor organs must undergo a period of cold ischemia during transport, exposure to warm ischemia is unique to DCD organs and may diminish the organ’s ability to tolerate subsequent cold ischemia (12). Injury to a transplanted organ as a result of a period of ischemia during procurement followed by reinitiation of blood flow through the organ after the transplant is referred to as ischemia-reperfusion injury (IRI). Studies have demonstrated that DCD kidneys/organs are more susceptible to IRI than SCD organs (13, 14).

Ischemia-reperfusion injury is a complex process that is incompletely understood. After removal of an organ from a donor, the ischemic injury is sustained when tissues are depleted of oxygen and nutrients and metabolic waste accumulates (15). IRI is characterized as a complicated process in which multiple mechanisms appear to play a role including tissue hypoxia, oxidative injury, inflammatory response, and apoptosis (16–19). Due to impaired aerobic metabolism, heme oxygenase-1 becomes overwhelmed and iron-containing compounds collect in the cytosol. These compounds catalyze free radical-generating

reactions. Following kidney transplantation, the level of inducible NOS (iNOS) has been shown to be upregulated due to IRI (20), leading to the production high levels of nitric oxide and formation of peroxynitrite, a powerful oxidant that contributes to damage of the cytoskeleton and cell membrane and is associated with proximal tubular cell detachment (10, 15). Other explanations for ischemic injury include decreased cellular pH and increased lytic enzyme activation due to the stimulation of anaerobic metabolism as well as reduced expression of genes that protect against ischemia in cadaveric kidneys (15).

After reperfusion, the additional injury is sustained due to stimulation of the host immune response and further production of reactive oxygen species. Proximal tubule cells release pro-inflammatory cytokines, such as IL-6 and TNF-α (10). Increased production of other cytokines including TGF-β, IFN-γ, and IL-10 may also increase the expression of MHC class I and II molecules in the graft leading to increased allograft immunogenicity and an increased risk of acute rejection (15, 21). Another potential contributing factor is that donor dendritic cells may respond to hypoxia and hypotension by migrating out of the allograft and into the recipient's lymphoid tissue, activating the recipient's adaptive immune system. The consequent influx of lymphocytes into the graft may cause vascular congestion, activation of the complement system and clotting cascade, and thrombosis (10).

Nitric oxide (NO), a bioactive gas produced at low levels by the constitutive NOS isoforms by several cell types including endothelial cells, has been shown to be involved in many biological functions that promote tissue perfusion and limit inflammation, which consequently provides a cytoprotective element against ischemic damages (22). Thrombospondin-1 (TSP-1) protein is a soluble ligand of the CD47 receptor that can be secreted by cells throughout the vascular system in response to hypoxia, thrombosis and other stresses (23). The TSP-1/CD47 interaction results in inhibition of NO signaling via down-regulating of the guanylyl cyclase activation, production of cyclic guanosine monophosphate (cGMP), and protein kinase G activation (24). Furthermore, in mice either lacking CD47 or following anti-CD47 antibody treatment, the NO signaling pathway is enhanced resulting in reduced oxidative injury and inflammatory responses in several models of IRI (22, 23). Blockade of the CD47 receptor also provides protection against IRI that occurs following transplantation by promoting vasodilation and improving blood flow to renal grafts as demonstrated in our previous study. CD47 blockade significantly reduced the histological damage of rat kidney transplants, promoted renal tubular cell self-renewal (25), and consequently improved graft survival after kidney transplantation using SCD grafts (26). In our previous studies, we also found that CD47 blockade protected both lean and steatotic rat liver grafts from IRI following liver transplantation (27, 28).

Taken together, we hypothesize that treatment of kidney grafts with antibody-mediated CD47 receptor blockade may attenuate IRI and improve the function of DCD organs after transplantation in a porcine large animal model.

Materials and Methods

Animals

Female Landrace pigs (30–35kg) were obtained from Oak Hill Genetics of Illinois and were allowed to acclimate for 72 hours before the experiments. Food and water were available *ad libitum*. Animals were fasted from solid food 12 hours before the kidney transplantation. All experimental procedures and protocols were approved by the Animal Studies Committee and Department of Comparative Medicine at Washington University School of Medicine in St Louis and performed according to the National Resource Council guidelines.

Perioperative treatments, procurement, and implantation of pig renal allografts of donation after cardiac death (DCD)

All animals were treated with buprenorphine 0.005–0.1mg/kg and a TKX cocktail (Telazol 4mg/kg, ketamine 2mg/kg, and xylazine 2mg/kg) by intramuscular injection, intubated, and the anesthesia was maintained with 2.5% to 4% isoflurane in oxygen at a flow of 2.0 L/minute. The animals were subsequently prepared and draped sterilely, and an abdominal midline approach was used to access to the kidneys and vasculature. The core temperature of the animals were maintained around 37.5 °C for the procedure.

The donor was heparinized (150 unit/kg) and the aorta was cannulated. Cardiac arrest was induced using KCl (75–100 mg/kg). After 30 min of warm ischemia, the kidneys were flushed with 3L Custodial Histidine-Tryptophan-Ketoglutarate (HTK) solution (Dr. Franz Kohler Chemie Co.) and stored at 4°C for 3.5 hours. Just prior to implantation, the grafts were flushed either with control (n=4) or a humanized CD47mAb (clone anti-CD47 649, Tioma Therapeutics, Inc, St. Louis, n=4) at a dosage of 10 mg per 250–300 g kidney. This dosage was derived from our previous investigation in a rodent kidney transplant model (26). The flush was performed through the renal artery, and the effluent was flushed back through the organ 5 times to facilitate antibody exposure and binding to the endothelium.

For the recipient operation, a right neck incision to expose the external jugular vein was performed for the placement of a central line. After abdominal access was obtained, the small bowel was retracted, and the infrarenal vena cava (IVC), aorta, right iliac artery, and right iliac vein were dissected free. The vasculature of donor kidney was anastomosed to the recipient's IVC and right iliac artery in an end-to-side manner. After renal graft revascularization, both native kidneys were removed, and an extravesical ureteroneocystostomy was created. The abdominal fascia was closed with running and interrupted 0 PDS sutures, and the skin closed with interrupted 2-0 nylon suture. Blood loss during the surgery was less than 50mL. After the closure of the abdomen, the pigs were allowed to recover from anesthesia and then moved to a large animal facility to continue the post-transplant monitoring and care. The recipients were visited at least 3 times daily, and the venous blood gas was tested at each visit from post-operative days (POD) 0 through 5. The recipients received 500mL normal saline three times daily from POD 0 through 3. The recipients also received analgesics (Buprenex, 0.20 mg/kg/TID, IM), antibiotics (Baytril, 4mg/kg/day, IV), and immunosuppressants (tacrolimus, 0.13 mg/kg/day, P.O. in two divided doses; mycophenolate, 16.66 mg/kg/day, P.O. in two divided doses; Solu-Medrol, 8.33

mg/kg on day 0, tapered down to 0.26 mg/kg until day 5). Blood samples were collected daily at the first daily visit prior to IV fluid and medication administration.

In vivo imaging study of the reperfusion renal DCD grafts

The SPY image system (NOVADAQ, BC, Canada) was used to assess the reperfusion of renal grafts. After the vascular anastomoses were made and before reperfusion, the recording was initiated and indocyanine green (ICG, 0.02 mg/kg) was infused through the central venous catheter followed by 10mL of saline. The ICG was allowed to circulate for one minute, and then the clamps were released to allow reperfusion of the graft. The SPY Elite camera was suspending over the field to image blood flow into the graft for 90 seconds. The images of grafts blood flow prior (0s) and post reperfusions at 1s, 15s, 30s, and 60s were exported, and the fluorescence density was extracted to analyze the reperfusion. The fluorescence density of the region of interest (ROI) was extracted to evaluate the grafts reperfusion after the renal vasculature were anastomosed and clamps were released using a similar method as previously reported (29).

The imaging data had 501 fluorescence density values for each pig. Data was collected on four pigs, two in the control group and two in the treatment group, over five time points (i.e., 0s, 1s, 15s, 30s, and 60s). A repeated measure two-way ANOVA was conducted to examine the time, treatment, and interaction of time and treatment effects on the fluorescence density, where a generalized estimating equation (GEE) approach was used to estimate the model parameters assuming an exchangeable covariance structure, given that there might be unknown correlations between observed fluorescence density values within the same pig. Multiple comparisons across treatment and time was adjusted by Tukey-Kramer method. This statistical analyses were performed using SAS version 9.4 (SAS Institute, Cary, NC).

Sampling, serum chemistry, enzyme-linked immunosorbent assay (ELISA) analysis and in vitro antibody binding to RBCs

Blood samples of the recipients were collected from day 0 to postoperative day 5. The recipient animals were euthanized on postoperative day 5 or 6, at which time, the graft was recovered, and portions were preserved in formalin or snap frozen in liquid nitrogen for further analysis. Serum creatinine, blood urea nitrogen, and potassium were measured daily using the LIASYS clinical chemistry system (AMS diagnostics LLC) and blood gas was measured by the Stat Profile pHOx plus C system (Nova biomedical) at least three times per day. ELISA analyses of IL-6 (ESIL6, Thermofisher), TNF-α (ab100756, Abcam), IL-10 (KSC0101, Thermofisher), and TGF-β1 (437707, Biolegend) were performed according to the manufacturer's instructions.

To assess binding of the CD47mAb to porcine red blood cells (RBCs), freshly obtained blood was diluted 1/300 and RBCs were washed three times with PBS containing 1 mM EDTA (PBS/E). Washed RBCs were incubated with freshly diluted antibody, either the anti-CD47 649 or an isotype matched control antibody, in PBS/E (concentrations from 0.0003 to 10 μg/ml) for 60 min at 37°C. After two washes, cells were incubated with a fluorescein isothiocyanate (FITC)-labeled goat anti-human IgG (H+L) antibody (Jackson ImmunoResearch) for 60 min at 37 °C and then washed twice with PBS/E. To assess

antibody binding to RBCs, fluorescence was measured by flow cytometry using a C6 Accuri flow cytometer (Becton Dickinson). An apparent K_d was calculated using a non-linear curve fit with GraphPad Prism 6 (San Diego, CA).

Histological assessment, and immunofluorescence staining of the renal grafts

FFPE tissue was cut into a thickness of 5μm and Periodic acid-Schiff (PAS) staining done using a standard protocol. The histologic assessment of kidney injury after transplantation was performed by an experienced renal pathologist in a blinded fashion by a renal pathologist (J.P.G). Immunofluorescence (IF) staining was performed to detect various relevant proteins associated with inflammation, renal injury or cell death using the following antibodies: CD4 (451530, Southern Biotech), CD8 (ab4055, Abcam), voltage-dependent anion-selective channel protein 1 (VDAC-1; ab191440, Abcam), Poly (ADP-ribose) polymerase (PARP, ab194586, Abcam), matrix metalloproteinase-2 (MMP-2; orb101049, Biorbyt), and matrix metalloproteinase-9 (MMP-9; orb101739, Biorbyt), Bcl2-Associated X Protein (BAX; ABIN2705572, Biorbyt) and cleavage Caspase-3 (9661, CST). Briefly, renal tissue samples obtained on day 5 after transplantation were snap frozen in liquid nitrogen. Subsequently, the frozen tissue was cut into a thickness of 5μm and incubated with primary antibodies at 4 °C overnight, secondary antibody 1 hour at room temperature, and mounted with DAPI. To assess the binding of the humanized anti-CD47 monoclonal antibody to CD47 on various cell types in the kidney, renal tissue samples were obtained immediately after flushing in the cold CD47mAb solution or 5 days after transplant and were snap frozen in liquid nitrogen. Five μm sections were incubated with FITC-labeled secondary anti-human IgG antibody (1:300) for 1 hour at room temperature, and mounted with DAPI. Photomicrographs were taken with Zeiss Observer Z1 immunofluorescence microscope and images were captured by Axiovision 4.8.2 software.

Western blotting and real-time quantitative reverse transcription polymerase chain reaction (qRT-PCR)

Protein lysis was performed at 4°C to prevent proteolytic degradation of the total proteins. Approximately 100mg of frozen tissue was homogenized using a homogenizer 3 times for 10 seconds each in 10 volumes of RIPA lysis buffer with proteases and phosphorylase cocktail inhibitors. The homogenates were centrifuged for 5 minutes at 10,000 rpm at 4°C to pellet the nuclei and particular matter. Protein concentrations of supernatants were measured using an Invitrogen kit (Q33211, Invitrogen). Prepared homogenates were aliquoted and stored at −80°C until use. For each sample, 50 μg/well of total protein lysate was loaded onto a 4–12% Nu-PAGE Bis-Tris (Invitrogen) gel and subjected to 2 hours of electrophoresis at 80 V. The proteins were then transferred from the gels to PVDF membranes (1620177, BIO-RAD) in a semidry apparatus at 30 V for 1.5 hours. The membranes were blocked with 5% milk and incubated with primary antibodies, diluted 1:1000, and overnight at 4°C. The primary antibodies used for western blots were the same as used for immunofluorescence staining. To demonstrate the specificity of CD47mAb binding, the humanized CD47mAb was used as primary antibody to perform Western blots. In addition, an anti-SIRP-alpha (DCABY-350, Creative Diagnostics) and an anti-TSP-1 (MA5-13398) were also used. Blots were washed and incubated with secondary antibodies (horseradish peroxidase conjugated goat anti-rabbit (7074S, CST) and goat anti-mouse

immunoglobulins (7076S, CST)) diluted at 1:2000 for 1 hour at room temperature. Membranes were developed with an ECL Kit (6883S, CST) for various times.

For qPCR analysis, total mRNA was isolated by using the Qiagen RNeasy Mini Kit (74104, Qiagen) according to the manufacture's protocol. The mRNA concentrations were measured with Qubit assays (Q32852, Invitrogen). cDNA was created from reverse transcription of 1.0μg of total RNA (205311, Qiagen). The cDNA samples were analyzed by the qRT-PCR. Each 10μL PCR reaction mix contained: 5μL TaqMan fast master mix, 0.5μL assay mix, 1μL sample, 3.5μL H_2O. The assay mixes of superoxide *dismutase*-1 (*sod-1,* Ss03375614_u1), *glutathione peroxidase-1* (*gpx-1,* Ss03383336_u1), *thioredoxin* (*txn,* Ss03222879_m1), *heme oxygenase-1* (*hmo-1,* Ss03378516_u1), *interleukin-2* (*il-2,* Ss03392428_m1), *interleukin-4* (*il-4,* Ss03394125_m1), interleukin-6 (*il-6,* Ss03384604_u1), *interferon gamma* (*ifn-g,* Ss03391054_m1), *transforming growth factor-beta* (*tgf-b,* Ss03382325_u1), *tumor necrosis factor alpha* (*tnf-a,* Ss03391318_g1), and GAPDH (Ss03374854_g1) were purchased from Thermo Fisher scientific. The samples were examined in duplicate and GAPDH was used as housekeeping gene. qPCR was performed on an ABI prism 7000 machine. In the linear range of the amplification, amplification curves were analyzed to obtain the cycle threshold (Ct) value. All genes expressions were normalized to the housekeeping gene, and fold change of expressions were calculated using delta (delta Ct) value methods.

Statistical Analysis

GraphPad Prism 5 software (San Diego, CA) was used to generate graphs. Data are presented as mean ± SD. Student's *t*-test was used to compare the differences between studying groups. p-values less than 0.05 were considered significant.

Results

Humanized CD47mAb strongly bound to the donor kidney tissue and increased the reperfusion of the renal allografts

The Landrace pig model of kidney transplantation (KTx) in bilaterally-nephrectomized recipient animals using DCD kidneys was used to investigate the effects of CD47 blockade on allograft function. We determined that 30 minutes of warm ischemia time (WIT) after circulatory arrest in the donor animals induced significant renal damage, but that was consistent with survival of the recipient animals for the 5-day duration of the study. The antibody was administered to the donor organ by perfusing the allograft with the CD47mAb diluted in cold HTK solution just prior to implantation. Control kidneys were perfused with cold HTK. To assess the binding characteristics of the antibody, we performed a set of experiments in which kidneys were treated with CD47mAb or HTK, transplanted, and then recovered several hours later. The CD47mAb bound to the kidney tissue, localized with FITC-labelled anti-human antibodies, showed that the CD47mAb was specifically bound to the pig kidney tissue, while no signal was detected in the kidneys perfused with HTK without antibody (Figure 1A). Residual CD47mAb binding to the glomerulus was still detected in grafts recovered from animals 5 days following transplant (Figure 1B). CD47mAb binding experiments. Furthermore, Western blots results showed that the protein

bound by the humanized CD47mAb was distinct from SIRP-alpha and TSP-1 in the pig kidney and liver, suggesting the CD47mAb binding was specific (Figure S1A). In addition, we performed an *in vitro* RBC binding assay and showed using flow cytometry that the CD47mAb bound in a concentration-dependent manner with an apparent binding constant of approximately 30 pM (Figure S1B).

To assess the effect of CD47 blockade on reperfusion dynamics, we used an *in vivo* imaging technique that uses ICG fluorescence in the blood as a measure of blood flow (29). After the anastomoses of the graft were performed, ICG was administered intravenously, and then the vascular clamps were released. ICG fluorescence into the graft was then recorded as a video that could be analyzed (Figure 2A and Figure S1). A repeated measure two-way ANOVA shows that time ($p<0.0001$), treatment ($p=0.0023$), and interaction ($p<0.0001$) terms were all significant, indicating that the florescence density differed by treatment group and over time, and that the difference between treatment group was not constant over time (Figure 2B and 2C). These results suggest that CD47 blockade can significantly improve graft reperfusion dynamics.

CD47 receptor blockade improved DCD kidney function and minimized acute tubular injury after transplantation

Compared to the control, the CD47mAb treatment significantly reduced the elevated serum creatinine (Cr; Day 2: 5.27±0.82 vs 7.52+0.85, $p=0.003$; Day 3: 4.40±0.16 vs 8.83±1.75, $p=0.001$; Day 4: 3.13±0.68 vs 5.86±1.57, $p=0.012$; Day 5: 2.03±0.64 vs 3.73±1.24, $p=0.037$), blood urea nitrogen (BUN; Day 3: 76.75±17.88 vs 112.33±15.93, $p=0.011$; Day 4: 51.00±9.45 vs 87.67±10.63, $p<0.001$; Day 5: 29.01±7.39 vs 55.17±17.51, $p=0.024$) and phosphorus levels after kidney transplantation. By postoperative date 2 or 3 until the end of the study (5 days following transplant), the animals with CD47mAb treated grafts had lower serum levels of Cr and BUN, respectively (Figure 3A). The antibody therapy also prevented the reduction of and normalized the serum calcium levels after transplantation. The serum levels of potassium, sodium, chloride, and hematocrit (HCT) did not show significant differences between the antibody-treated and control groups (Figure S2A).

We performed histologic examination to assess the tissue injury in the grafts. Periodic acid-Schiff (PAS) staining of tissues from all grafts recovered at day 5 was performed and scored blindly for acute tubular injury by a renal pathologist. Grafts treated with CD47mAb showed significantly less acute tubular injury (ATI) than the control kidneys (Figure 3B, 5.7±3.3% vs 43.3±15.2%, $p=0.013$). During the postoperative care of the animals, the time of first urine output was recorded. We found that in these bilaterally nephrectomized animals, those receiving grafts treated with CD47mAb produced urine earlier than those the controls (15.0±5.0 vs 32.0±5.1 hours, $p<0.05$, Figure 3C).

Organs treated with CD47mAb had a diminished response to oxidative stress

To study the effects of CD47mAb treatment on oxidative stress in renal allografts after transplantation, we analyzed the expression of several genes related to oxidative stress at either the mRNA or protein levels. As shown in Figure 4A and compared to the DCD control, the CD47mAb treatment significantly reduced the relative mRNA expression of

superoxide dismutase-1 (*sod-1*, 0.61±0.16 vs 1.00±0.15, p=0.013), *glutathione peroxidase-1* (*gpx-1*, 0.64±0.05 vs 1.00±0.14, p=0.006), *thioredoxin* (*txn*, 0.34±0.15 vs 1.00±0.16, p=0.005), at day 5 after KTx. There was no significant change in expression of *heme oxygenase-1* (*hmox-1*) in the grafts between the treated and control groups. Immunofluorescence staining demonstrated that the CD47 blockade resulted in reduced staining of voltage-dependent anion-selective channel protein 1 (VDAC-1) and poly (ADP-ribose) polymerase-1 (PARP) in the glomerulus and renal tubular epithelial cells (Figure 4B). These observations were confirmed by western blotting and densitometry analysis, showing that CD47mAb treatment resulted in significantly less expression of VDAC-1(0.61±0.07 vs 1.09±0.06, p<0.001) and PARP (1.26±0.04 vs 1.44±0.06, p=0.003) in the CD47mAb-treated allografts than in the controls (Figure 4C and 4D, n=4/group).

The CD47mAb therapy decreased inflammatory response of DCD kidney after transplantation

We next assessed markers of the inflammatory response in the graft tissues. Using qRT-PCR and, we found that CD47mAb treatment significantly decreased the mRNA transcription of *interleukin-2* (*il-2*, 0.20±0.13 vs 1.00±0.28, p=0.002), interleukin-6 (*il-6*, 0.37±0.38 vs 1.00±0.19, p=0.026), *interferon gamma* (*ifn-g*, 0.34±0.13 vs 1.00±0.18, p=0.001) and *transforming growth factor-beta* (*tgf-b*, 0.54±0.25 vs 1.00±0.12, p=0.017) of the DCD renal grafts at day 5 after transplantation compared to the control grafts, while the mRNA levels of *interleukin-4* (*il-4*) and *tumor necrosis factor alpha* (*tnf-a)* remained unchanged (Figure 5A). Furthermore, Immunofluorescent staining showed the antibody treatment markedly lowered the $CD4^+$ (35.7±5.3 vs 66.2±9.4, p=0.001) and $CD8^+$ (11.7±4.1 vs 27.5±5.0, p=0.003) cells infiltration in the allografts compared with control at day 5 after KTx (Figure 5B).

CD47mAb treatment decreased apoptosis and renal architectural breakdown of DCD kidney after transplantation

To study the severity of tissue damage of the allografts, we assessed the expression of matrix metalloproteinase-2 (MMP-2), MMP-9, Bcl-2-associated X protein (BAX), and cleaved Caspase-3 by both immunofluorescence staining and western blotting analysis. We found that CD47mAb treatment reduced the expression of MMP-2 and MMP-9 in both the glomerulus and renal tubular epithelium of the renal graft tissue at day 5 post transplantation (Figure 6A). In support of the Immunohistochemical staining, western blotting and densitometry analysis demonstrated a significant decrease of MMP-2 (0.54±0.24 vs 0.91±0.08, p=0.002) and MMP-9 (0.42±0.16 vs 0.92±0.12, p<0.001) in the CD47mAb-treated group compared to the control (Figure 6B and 6C, n=4/group). In addition, the CD47mAb treatment also diminished the expression of BAX (0.72±0.35 vs 1.33±0.32, p=0.040) and cleaved Caspase-3 (0.99±0.22 vs 0.41 ± 0.18, p=0.006) in renal allografts compared to the control at day 5 after transplantation by both IHC and western analysis (Figure 7A–7C, n=4/group).

Discussion

In this study, we demonstrate that CD47 blockade with a monoclonal antibody provides significant protection of renal allografts in a DCD porcine large animal model of

transplantation and an increase of blood flow was measured at the early time of reperfusion in the CD47mAb treated allografts. In addition, we observed increased function (time to first urination), reduced renal injury (assessed by Cr and BUN), oxidative injury, inflammatory response, and apoptosis, and preservation of the renal architecture in the CD47mAb treated grafts compared to the controls. In this DCD model, we induced graft damage by subjecting the organs to 30 minutes of WIT after circulatory arrest. This is arguably more severe than the DCD procedure in the human setting, where the donor may have hypoxia and hypotension for a period of time, followed by 5 minutes of WIT after circulatory arrest. We had attempted to perform these studies with 60 minutes WIT, but by postoperative day 1, the serum potassium levels of control animals exceeded the allowed threshold allowed by the animal protocol and by our institutional Animal Studies Committee (Figure S2B). The hematocrit of animals receiving CD47mAb treated grafts trended lower, although this did not reach statistical significance (Figure S2B). This may be due to transient binding of the antibody to CD47 on red blood cells with subsequent clearance by the spleen. A transient anemia was also observed in rodent models using CD47 blockade with antibodies (30).

We assessed CD47mAb binding in the renal grafts immediately after cold perfusion and showed the CD47mAb strongly localized to the kidney tissue after flushing at 4°C, particularly to the glomeruli. The retention of some antibody binding, although lower, was also observed even 5 days after transplantation. Because of this ability to bind at 4°C, CD47mAb may be used in conjunction with hypothermic pumping, although this would need to be tested directly to show whether there are additive benefits to using both interventions.

Given the close interactions among CD47, Signal-regulatory protein-alpha (SIRP-alpha), and TSP-1, we performed assays to establish the binding specificities of the CD47mAb. Western blot analysis demonstrated that the humanized CD47mAb only recognized a protein of the predicted molecular weight of CD47 (55kD). This band was distinct from that of SIRP-alpha or TSP-1, suggesting this antibody binds specifically to CD47. In addition, we showed potent, concentration–dependent binding to porcine RBCs which express cell surface CD47.

Consistent with the well-established mechanism of vasodilation after CD47 blockade (23, 26, 31, 32), we also observed significant improvement in blood perfusion in the CD47mAb-treated renal allografts at the time of transplant using an *in vivo* imaging technique. Throughout the postoperative course, the serum indicators of renal injury, including creatinine and blood urea nitrogen, were lower in animals receiving CD47mAb-treated grafts. At the end of the experiment, the recovered grafts were examined for histologic evidence of renal tubular injury, and those treated with CD47mAb showed less histologic evidence of injury severity.

In addition, we examined other pathways of injury in the graft tissues. CD47mAb treatment profoundly reduced the oxidative stress and inflammatory responses in the tissues after transplantation. After re-establishment of blood perfusion and oxygen delivery to the tissues, reperfusion leads to production of reactive oxygen species that has been found to initiated a cascade of deleterious cellular responses leading to inflammation, cell death, and acute

kidney failure (16). In response, the up-regulation of genes encoding antioxidant enzymes, such as *superoxide dismutase-1 (sod-1), glutathione peroxidase-1 (gpx-1),* and *thioredoxin (txn)* have been found to be increased to counteract this oxidative stress (33, 34). We measured the magnitude of the oxidative stress response in the transplanted graft tissues and found that the ones treated with CD47mAb had significantly less evidence of oxidative stress. It has been shown that in CD47-null mice, mitochondria accumulated in a tissue-specific and age-dependent fashion that resulted in lowered reactive oxygen species production and enhanced physical performance (24). Indeed in the present study, we found a significant down-regulation of *sod-1, gpx-1,* and *txn* mRNA levels in the CD47mAb treated the group compared to the control group, suggesting the CD47 blockade reduced oxidative stress of the DCD renal grafts and thus the need for the compensatory upregulation of the antioxidant enzymes. *Hmo-1* mRNA expression was not different between the two groups which could be due to the dynamics of the oxidative stress response and our ability to assess only the day 5-time point. The serum calcium levels in the CD47 treated group were also significantly higher than in the control group, suggesting CD47mAb treatment stabilized calcium and phosphorus homeostasis possibly due to improved renal function. We also found that voltage-dependent anion-selective channel protein 1 (VDAC-1), an abundantly expressed calcium ion transport channel (35, 36), was significantly reduced in the CD47mAb treated animals compared to the DCD control animals suggesting that calcium influx was decreased in the CD47mAb treated allografts compared to controls. Furthermore, it has been shown that increased tubular expression of Poly ADP-Ribose polymerase-1 (PARP) has been associated with delayed graft function in expanded criteria donor (ECD) human kidney allografts and in non-ECD allografts that develop posttransplant acute tubular necrosis (37). We observed strong expression of PARP in the nucleus of both the renal tubular epithelium and glomeruli of the DCD grafts, but this expression was significantly reduced in the CD47mAb treated group as compared to the control group.

Numerous studies have shown that pro- and anti-inflammatory cytokines are released during the inflammatory response that accompanies IRI in transplanted organs (38–40). One potential strategy for reducing IRI is to target the inflammatory cascades at their early stages. CD47 blockade has been shown to inhibit IL-12-driven Th1 cell development (41) and IL-2 response of activated naive T cells (42). It also has been shown to suppress bacteria-induced production of IL-12, TNF-α, GM-CSF, and IL-6 by immature dendritic cells following exposure to microorganisms and limit the intensity and duration of the inflammatory response (43). In our study, we found that the transcription of *il-2*, *il-6*, *ifn-γ*, and *tgf-β* mRNA levels, as well as the infiltration of $CD4^+$ and $CD8^+$ cells in the allografts were significantly reduced by CD47mAb therapy. We were not, however, able to detect changes of these cytokines in the serum after CD47mAb treatment. Together, our data and previous studies (23, 31) from other groups suggest that CD47mAb treatment may reduce the inflammatory response in the DCD kidney grafts.

Matrix metalloproteinases (MMPs), particularly MMP-2 and MMP-9, are endopeptidases that degrade the extracellular matrix resulting in injury to ischemic organs and inhibitors of MMPs can decrease the reperfusion injury that occurs in ischemic organs (44–48). In our study, the extended warm ischemia time after circulatory arrest resulted in significant expression of MMP-2 and MMP-9. This suggests that metalloproteinase activity was

responsible, at least in part, for some of the degradation and destruction of the DCD control renal allografts. In contrast, the grafts treated with CD47mAb had significantly decreased MMP-2 and MMP-9 expression. Furthermore, the expression of cleaved caspase-3 and Bcl-2-associated X protein (BAX) was decreased in the CD47mAb treated grafts compared to the DCD control group, showing that CD47 blockade decreases apoptosis in the kidney tissues after transplantation.

Similar to other large animal studies, there are several limitations in the current study. Because of logistic difficulties of maintaining large animals over long periods, we limited our post-transplant follow-up for 5 post-operative days. We were therefore unable to assess the long-term effects of CD47 blockade on factors such as chronic rejection. Also, we were unable to assess the treatment effects of CD47 blockade with higher severity IR, such as with longer donor warm ischemic times. In the human patient care setting, dialysis can be used to bridge a recipient through the recovery phase of the allograft, but this would be prohibitively difficult in the porcine model.

In summary, our data clearly demonstrates that CD47mAb therapy administered to the renal graft by flush protected the DCD renal allografts against many of the deleterious effects of ischemia-reperfusion injury after transplantation, assessed both intra-operatively using *in vivo* organ imaging techniques and post-operatively using serum biochemical markers of renal injury. We also found molecular evidence that this improved renal function was associated with decreased oxidative injury, inflammatory response and cell death and tissue injury. These results support in a large animal porcine DCD model the use of CD47 blockade in the transplant setting. Its use in human kidney transplants with DCD organs has the potential to decrease rates of delayed graft function and improve overall transplant outcomes.

Supplementary Material

Refer to Web version on PubMed Central for supplementary material.

Acknowledgments

This project was funded in part by the Barnes-Jewish Hospital Foundation Project Award, Transplant Research Support and by the National Institutes of Health grant 5R44DK092078. The content is solely the responsibility of the authors and does necessarily represent the official views of the National Institutes of Health. We thank Tioma Therapeutics, Inc. for providing the CD47mAb and the Digestive Diseases Research Core Centers (DDRCC, NIDDK P30 DK052574) at WUSM for sharing equipment and core facility support. We appreciate the help from NOVADAQ Technologies (Burnaby, BC, Canada) for providing the NIR imaging system used in the study.

Abbreviations

ESRD	end-stage renal disease
KTx	Kidney transplantation
DCD	donation after cardiac death
IRI	ischemia reperfusion injury

DGF delayed graft function

CD47mAb CD47 monoclonal antibody

References

1. Wolfe RA, Ashby VB, Milford EL, Ojo AO, Ettenger RE, Agodoa LYC, et al. Comparison of Mortality in All Patients on Dialysis, Patients on Dialysis Awaiting Transplantation, and Recipients of a First Cadaveric Transplant. New England Journal of Medicine. 1999; 341(23):1725–1730. [PubMed: 10580071]
2. Merion RM, Ashby VB, Wolfe RA, et al. Deceased-donor characteristics and the survival benefit of kidney transplantation. JAMA. 2005; 294(21):2726–2733. [PubMed: 16333008]
3. USRDS Annual Data Report 2015: Epidemiology of Kidney Disease in the United States. Bethesda, Md: United States Renal Data System; 2015.
4. Matas AJ, Smith JM, Skeans MA, Thompson B, Gustafson SK, Schnitzler MA, et al. OPTN/SRTR 2012 Annual Data Report: Kidney. American Journal of Transplantation. 2014; 14(S1):11–44.
5. Overall by Organ: Current U.S. Waiting List. Organ Procurement and Transplantation Network, Health Resources and Services Administration, US Department of Health and Human Services; 2016. https://optn.transplant.hrsa.gov/data/view-data/reports/national-data/#
6. Heilman RL, Mathur A, Smith ML, Kaplan B, Reddy KS. Increasing the Use of Kidneys From Unconventional and High-Risk Deceased Donors. American Journal of Transplantation. 2016 n/a-n/a.
7. Stratta RJ, Farney AC, Orlando G, Farooq U, Al-Shraideh Y, Palanisamy A, et al. Dual kidney transplants from adult marginal donors successfully expand the limited deceased donor organ pool. Clinical transplantation. 2016; 30(4):380–392. [PubMed: 26782941]
8. Hart A, Smith JM, Skeans MA, Gustafson SK, Stewart DE, Cherikh WS, et al. Kidney. American Journal of Transplantation. 2016; 16(S2):11–46.
9. Locke JE, Segev DL, Warren DS, Dominici F, Simpkins CE, Montgomery RA. Outcomes of Kidneys from Donors After Cardiac Death: Implications for Allocation and Preservation. American Journal of Transplantation. 2007; 7(7):1797–1807. [PubMed: 17524076]
10. Siedlecki A, Irish W, Brennan DC. Delayed Graft Function in the Kidney Transplant. American journal of transplantation : official journal of the American Society of Transplantation and the American Society of Transplant Surgeons. 2011; 11(11):2279–2296.
11. Halazun KJ, Al-Mukhtar A, Aldouri A, Willis S, Ahmad N. Warm ischemia in transplantation: search for a consensus definition. Transplantation proceedings. 2007; 39(5):1329–1331. [PubMed: 17580133]
12. Summers DM, Johnson RJ, Hudson A, Collett D, Watson CJ, Bradley JA. Effect of donor age and cold storage time on outcome in recipients of kidneys donated after circulatory death in the UK: a cohort study. Lancet (London, England). 2013; 381(9868):727–734.
13. Rao PS, Ojo A. The alphabet soup of kidney transplantation: SCD, DCD, ECD--fundamentals for the practicing nephrologist. Clinical journal of the American Society of Nephrology : CJASN. 2009; 4(11):1827–1831. [PubMed: 19808229]
14. Tennankore KK, Kim SJ, Alwayn IP, Kiberd BA. Prolonged warm ischemia time is associated with graft failure and mortality after kidney transplantation. Kidney international. 2016; 89(3):648–658. [PubMed: 26880458]
15. Perico N, Cattaneo D, Sayegh MH, Remuzzi G. Delayed graft function in kidney transplantation. Lancet (London, England). 2004; 364(9447):1814–1827.
16. Malek M, Nematbakhsh M. Renal ischemia/reperfusion injury; from pathophysiology to treatment. Journal of renal injury prevention. 2015; 4(2):20–27. [PubMed: 26060833]
17. Faubel S, Ljubanovic D, Poole B, Dursun B, He Z, Cushing S, et al. Peripheral CD4 T-cell depletion is not sufficient to prevent ischemic acute renal failure. Transplantation. 2005; 80(5): 643–649. [PubMed: 16177639]
18. Burne-Taney MJ, Yokota N, Rabb H. Persistent renal and extrarenal immune changes after severe ischemic injury. Kidney international. 2005; 67(3):1002–1009. [PubMed: 15698438]

19. Martina MN, Noel S, Bandapalle S, Hamad AR, Rabb H. T lymphocytes and acute kidney injury: update. Nephron Clinical practice. 2014; 127(1–4):51–55. [PubMed: 25343821]
20. Noiri E, Peresleni T, Miller F, Goligorsky MS. In vivo targeting of inducible NO synthase with oligodeoxynucleotides protects rat kidney against ischemia. The Journal of clinical investigation. 1996; 97(10):2377–2383. [PubMed: 8636419]
21. Xu M, Tan C, Zhou J, Huang X, Dai Z, Zhu H, et al. The dynamic changes of T-bet+/GATA-3+ and RORγt+/FOXP3+ cells in recipient spleens and grafts after rat orthotopic liver transplantation. Transplant immunology. 2010; 22(3):165–171. [PubMed: 19922796]
22. Phillips L, Toledo AH, Lopez-Neblina F, Anaya-Prado R, Toledo-Pereyra LH. Nitric oxide mechanism of protection in ischemia and reperfusion injury. Journal of investigative surgery : the official journal of the Academy of Surgical Research. 2009; 22(1):46–55. [PubMed: 19191157]
23. Rogers NM, Thomson AW, Isenberg JS. Activation of parenchymal CD47 promotes renal ischemia-reperfusion injury. Journal of the American Society of Nephrology : JASN. 2012; 23(9): 1538–1550. [PubMed: 22859854]
24. Frazier EP, Isenberg JS, Shiva S, Zhao L, Schlesinger P, Dimitry J, et al. Age-dependent regulation of skeletal muscle mitochondria by the thrombospondin-1 receptor CD47. Matrix biology : journal of the International Society for Matrix Biology. 2011; 30(2):154–161. [PubMed: 21256215]
25. Rogers NM, Zhang ZJ, Wang JJ, Thomson AW, Isenberg JS. CD47 regulates renal tubular epithelial cell self-renewal and proliferation following renal ischemia reperfusion. Kidney international. 2016; 90(2):334–347. [PubMed: 27259369]
26. Lin Y, Manning PT, Jia J, Gaut JP, Xiao Z, Capoccia BJ, et al. CD47 blockade reduces ischemia-reperfusion injury and improves outcomes in a rat kidney transplant model. Transplantation. 2014; 98(4):394–401. [PubMed: 24983310]
27. Xiao ZY, Banan B, Jia J, Manning PT, Hiebsch RR, Gunasekaran M, et al. CD47 blockade reduces ischemia/reperfusion injury and improves survival in a rat liver transplantation model. Liver Transpl. 2015; 21(4):468–477. [PubMed: 25482981]
28. Xiao Z, Banan B, Xu M, Jia J, Manning PT, Hiebsch RR, et al. Attenuation of Ischemia-Reperfusion Injury and Improvement of Survival in Recipients of Steatotic Rat Livers Using CD47 Monoclonal Antibody. Transplantation. 2016; 100(7):1480–1489. [PubMed: 27331362]
29. Levinson KL, Mahdi H, Escobar PF. Feasibility and optimal dosage of indocyanine green fluorescence for sentinel lymph node detection using robotic single-site instrumentation: preclinical study. Journal of minimally invasive gynecology. 2013; 20(5):691–696. [PubMed: 24034538]
30. Willingham SB, Volkmer J-PJ-P, Gentles AJ, Sahoo D, Dalerba P, Mitra SS, et al. The CD47-signal regulatory protein alpha (SIRPa) interaction is a therapeutic target for human solid tumors. Proceedings of the National Academy of Sciences of the United States of America. 2012; 109:6662–6667. [PubMed: 22451913]
31. Rogers NM, Yao M, Novelli EM, Thomson AW, Roberts DD, Isenberg JS. Activated CD47 regulates multiple vascular and stress responses: implications for acute kidney injury and its management. American journal of physiology Renal physiology. 2012; 303(8):F1117–1125. [PubMed: 22874763]
32. Yao M, Rogers NM, Csanyi G, Rodriguez AI, Ross MA, St Croix C, et al. Thrombospondin-1 activation of signal-regulatory protein-alpha stimulates reactive oxygen species production and promotes renal ischemia reperfusion injury. Journal of the American Society of Nephrology : JASN. 2014; 25(6):1171–1186. [PubMed: 24511121]
33. Chang MW, Chen CH, Chen YC, Wu YC, Zhen YY, Leu S, et al. Sitagliptin protects rat kidneys from acute ischemia-reperfusion injury via upregulation of GLP-1 and GLP-1 receptors. Acta pharmacologica Sinica. 2015; 36(1):119–130. [PubMed: 25500876]
34. Singh I, Gulati S, Orak JK, Singh AK. Expression of antioxidant enzymes in rat kidney during ischemia-reperfusion injury. Molecular and cellular biochemistry. 1993; 125(2):97–104. [PubMed: 8283974]
35. De Pinto V, Guarino F, Guarnera A, Messina A, Reina S, Tomasello FM, et al. Characterization of human VDAC isoforms: a peculiar function for VDAC3? Biochimica et biophysica acta. 2010; 1797(6–7):1268–1275. [PubMed: 20138821]

36. Chu Y, Goldman JG, Kelly L, He Y, Waliczek T, Kordower JH. Abnormal alpha-synuclein reduces nigral voltage-dependent anion channel 1 in sporadic and experimental Parkinson's disease. Neurobiology of disease. 2014; 69:1–14. [PubMed: 24825319]
37. O'Valle F, Del Moral RG, del Benitez MC, Martin-Oliva D, Gomez-Morales M, Aguilar D, et al. Poly[ADP-ribose] polymerase-1 expression is related to cold ischemia, acute tubular necrosis, and delayed renal function in kidney transplantation. PloS one. 2009; 4(9):e7138. [PubMed: 19784367]
38. Takada M, Nadeau KC, Shaw GD, Marquette KA, Tilney NL. The cytokine-adhesion molecule cascade in ischemia/reperfusion injury of the rat kidney. Inhibition by a soluble P-selectin ligand. The Journal of clinical investigation. 1997; 99(11):2682–2690. [PubMed: 9169498]
39. Bihorac A, Baslanti TO, Cuenca AG, Hobson CE, Ang D, Efron PA, et al. Acute kidney injury is associated with early cytokine changes after trauma. The journal of trauma and acute care surgery. 2013; 74(4):1005–1013. [PubMed: 23511138]
40. Hahn AB, Kasten-Jolly JC, Constantino DM, Graffunder E, Singh TP, Shen GK, et al. TNF-alpha, IL-6, IFN-gamma, and IL-10 gene expression polymorphisms and the IL-4 receptor alpha-chain variant Q576R: effects on renal allograft outcome. Transplantation. 2001; 72(4):660–665. [PubMed: 11544427]
41. Avice MN, Rubio M, Sergerie M, Delespesse G, Sarfati M. CD47 ligation selectively inhibits the development of human naive T cells into Th1 effectors. Journal of immunology (Baltimore, Md : 1950). 2000; 165(8):4624–4631.
42. Avice MN, Rubio M, Sergerie M, Delespesse G, Sarfati M. Role of CD47 in the induction of human naive T cell anergy. Journal of immunology (Baltimore, Md : 1950). 2001; 167(5):2459–2468.
43. Demeure CE, Tanaka H, Mateo V, Rubio M, Delespesse G, Sarfati M. CD47 engagement inhibits cytokine production and maturation of human dendritic cells. Journal of immunology (Baltimore, Md : 1950). 2000; 164(4):2193–2199.
44. Kunugi S, Shimizu A, Kuwahara N, Du X, Takahashi M, Terasaki Y, et al. Inhibition of matrix metalloproteinases reduces ischemia-reperfusion acute kidney injury. Laboratory investigation; a journal of technical methods and pathology. 2011; 91(2):170–180. [PubMed: 20956976]
45. Moser MA, Arcand S, Lin HB, Wojnarowicz C, Sawicka J, Banerjee T, et al. Protection of the Transplant Kidney from Preservation Injury by Inhibition of Matrix Metalloproteinases. PloS one. 2016; 11(6):e0157508. [PubMed: 27327879]
46. Iwata T, Chiyo M, Yoshida S, Smith GN Jr, Mickler EA, Presson R Jr, et al. Lung transplant ischemia reperfusion injury: metalloprotease inhibition down-regulates exposure of type V collagen, growth-related oncogene-induced neutrophil chemotaxis, and tumor necrosis factor-alpha expression. Transplantation. 2008; 85(3):417–426. [PubMed: 18322435]
47. Padrissa-Altes S, Zaouali MA, Franco-Gou R, Bartrons R, Boillot O, Rimola A, et al. Matrix metalloproteinase 2 in reduced-size liver transplantation: beyond the matrix. American journal of transplantation : official journal of the American Society of Transplantation and the American Society of Transplant Surgeons. 2010; 10(5):1167–1177.
48. Soccal PM, Gasche Y, Miniati DN, Hoyt G, Berry GJ, Doyle RL, et al. Matrix metalloproteinase inhibition decreases ischemia-reperfusion injury after lung transplantation. American journal of transplantation : official journal of the American Society of Transplantation and the American Society of Transplant Surgeons. 2004; 4(1):41–50.

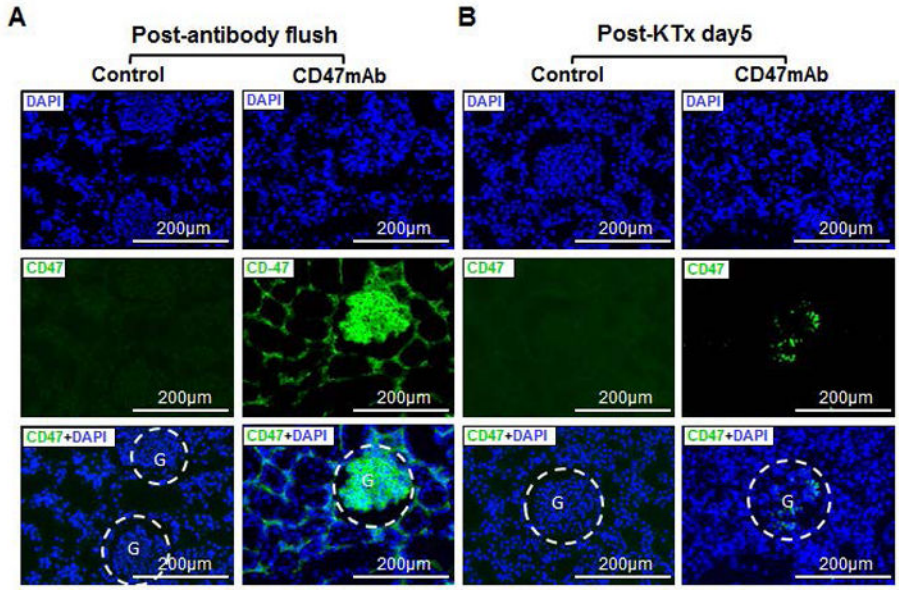

Figure 1. Immunohistochemical localization of the antibody binding in the renal allografts pretreated with CD47mAb

(A) The CD47mAb was strongly bound to the renal tissue immediately after flushing. (B) CD47mAb binding to glomeruli could be detected on day 5 after transplant. (These staining were performed on grafts from different animals.)

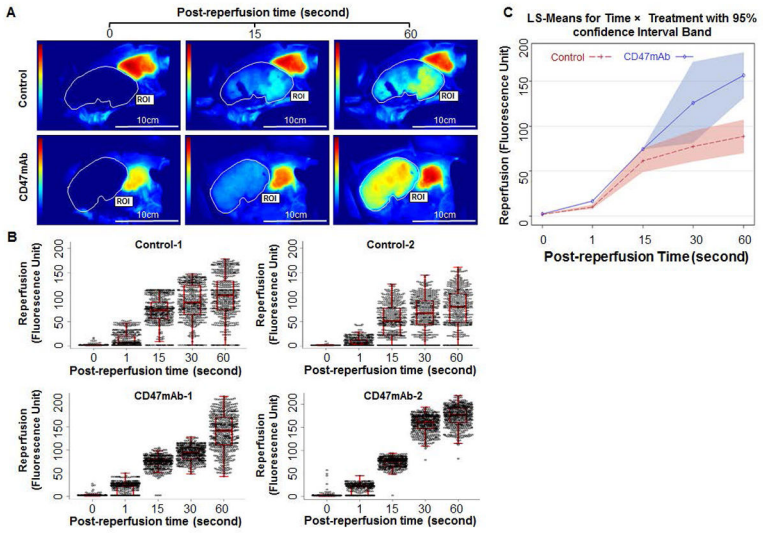

Figure 2. CD47mAb treatment resulted in more uniform and greater perfusion of DCD renal allografts

Graft blood flow prior (0s) and post reperfusions at 1s, 15s, 30s, and 60s were studied using an in *vivo* imaging system (n=2/group). (A) Representative perfusion using ICG fluorescence imaging are shown at time points 0, 16 and 60 seconds after release of clamps (see Figure S1 for additional images). (B) The fluorescence density values of the region of interest (ROI) were extracted to evaluate reperfusion characteristics of the grafts. CD47mAb-treated grafts had more uniform and greater average tissue perfusion as compared to control organs. (C) The repeated measure two-way ANOVA shows that Time ($p<0.001$), Treatment ($p=0.002$), and Interaction ($p<0.001$) terms are all significant, indicating florescent density differed by treatment and over time.

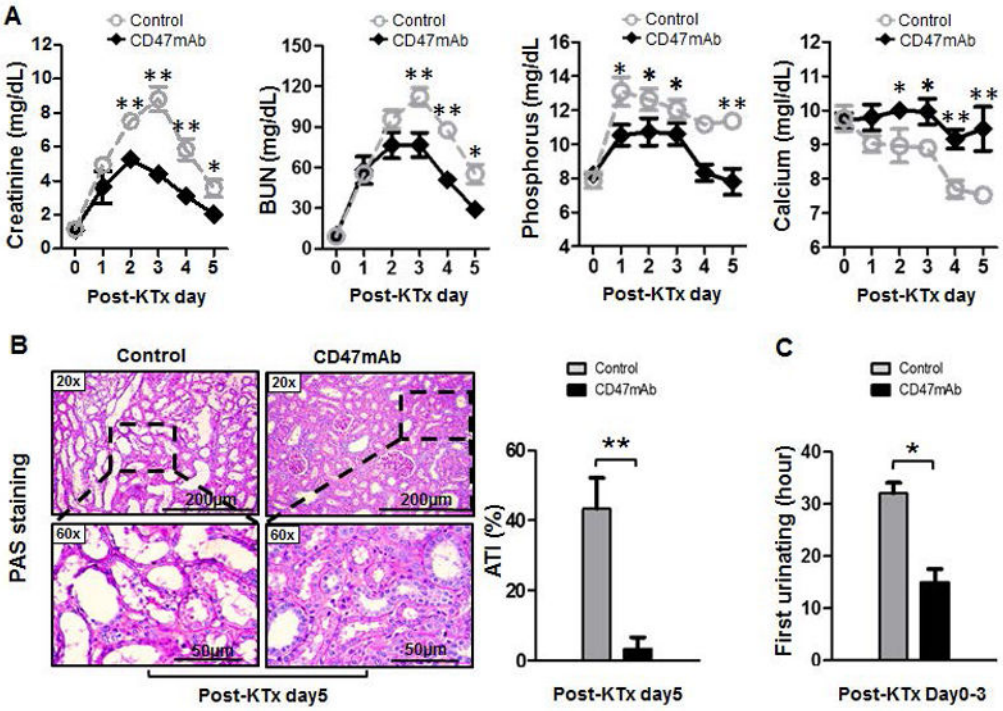

Figure 3. CD47mAb treatment improved the function of DCD renal allografts

(A) Serum creatinine, blood urea nitrogen (BUN), and phosphorus were significantly decreased, while the calcium levels were significantly increased in the CD47mAb-treated group than that in the control group. (B) Histological study of pig kidney grafts at day 5 post-KTx indicated that CD47mAb treated grafts had significantly less evidence of acute tubular injury (ATI) compared with the control group. (C) Animals with CD47mAb treated grafts had significantly earlier urination than that in control (n=4/group, CD47mAb treatment versus control, *p<0.05 or **p<0.01, respectively).

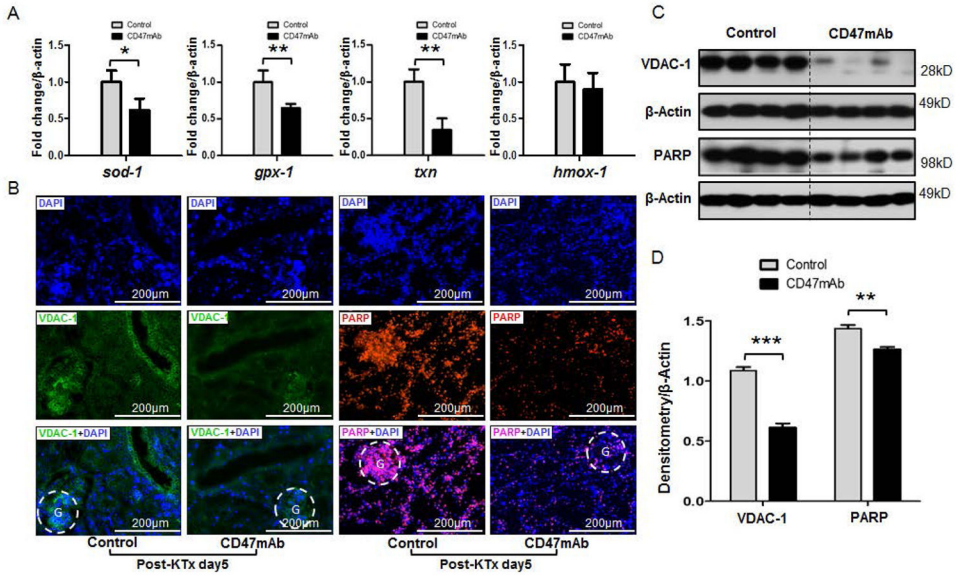

Figure 4. CD47mAb treatment reduced oxidative injury of DCD renal allografts

(A) Revealed by qRT-PCR, CD47mAb-treated organs showed significantly less expression in each of these oxidative injury-related genes of *superoxide dismutase-1* (*sod-1*), *glutathione peroxidase-1* (*gpx-1*), *thioredoxin* (*txn*), except *heme oxygenase-1* (*hmox-1*) compared to control. (B) Immunofluorescence staining revealed a decreased expression of Voltage-dependent anion-selective channel protein 1 (VDAC-1) and poly (ADP-ribose) polymerase (PARP) in the CD47mAb-treated tissues than in control. (C) Western blotting and (D) densitometry analysis also support that the protein levels of VDAC-1 and PARP are decreased in the grafts treated with CD47mAb compared with control (n=4/group, *p<0.05, ** p<0.01, or *** p<0.001, respectively).

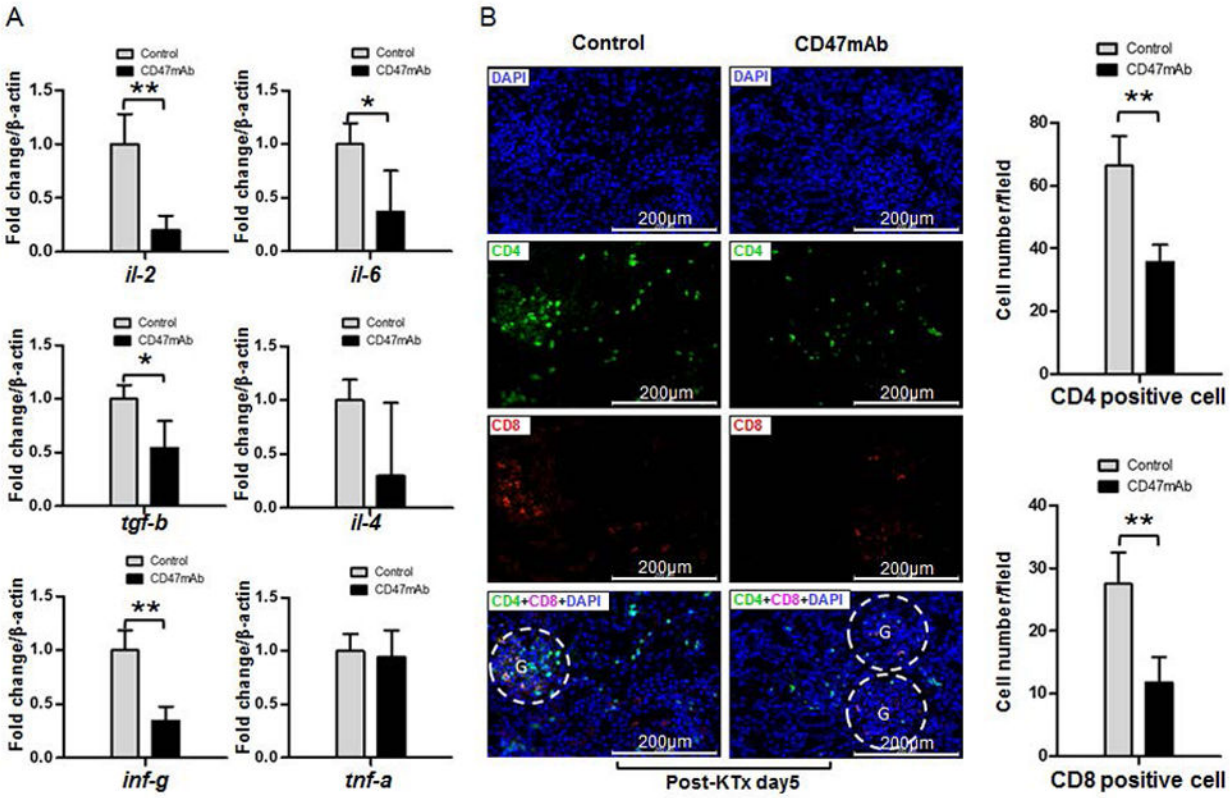

Figure 5. CD47mAb treatment decreased inflammatory response of the DCD renal grafts

(A) qRT-PCR showed the relative mRNA levels of *il-2*, *il-6*, *tgf-b*, and *inf-g* were significantly lower in the CD47mAb treated renal allografts than that in control at day 5 after kidney transplantation. (B) Immunofluorescence staining indicated the $CD4^+$ and $CD8^+$ cells infiltration were significantly decreased in the CD47mAb treated renal allografts than that in the control (n=4/group, *p<0.05 or ** p<0.01, respectively).

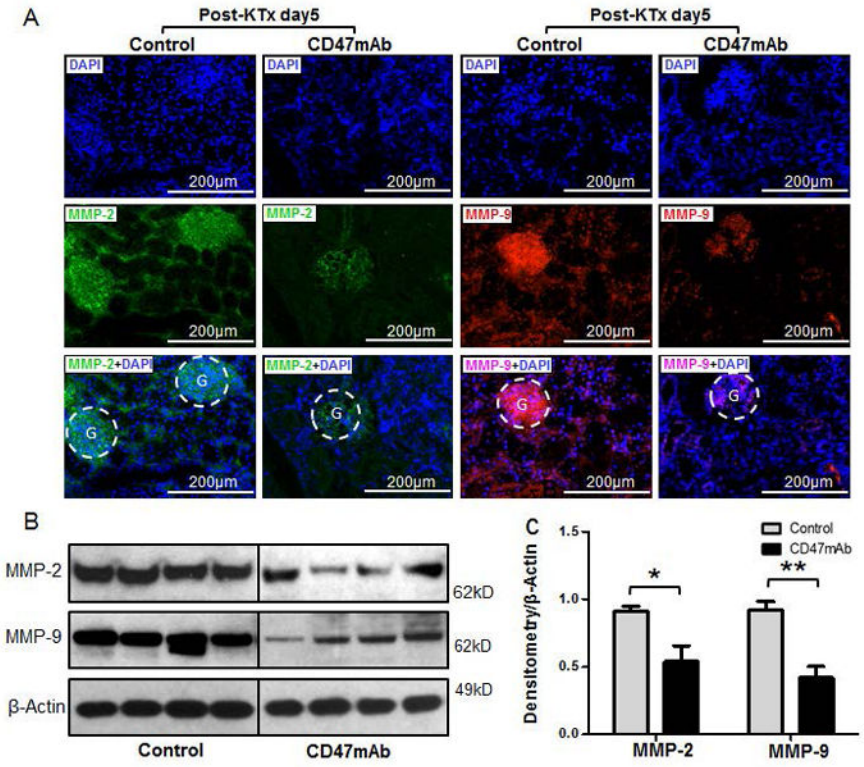

Figure 6. CD47mAb treatment diminished the structural destruction of DCD allografts after transplantation

(A) Immunofluorescence staining showed a reduction of matrix metalloproteinase-2 (MMP-2) and MMP-9 in CD47mAb treated renal allografts than that in control. Western blotting (B) and densitometry analysis (C) confirmed the decreasing expression of MMP-2 and MMP-9 in renal grafts treated with CD47mAb compared to control (n=4/group, *$p<0.05$ or ** $p<0.01$, respectively).

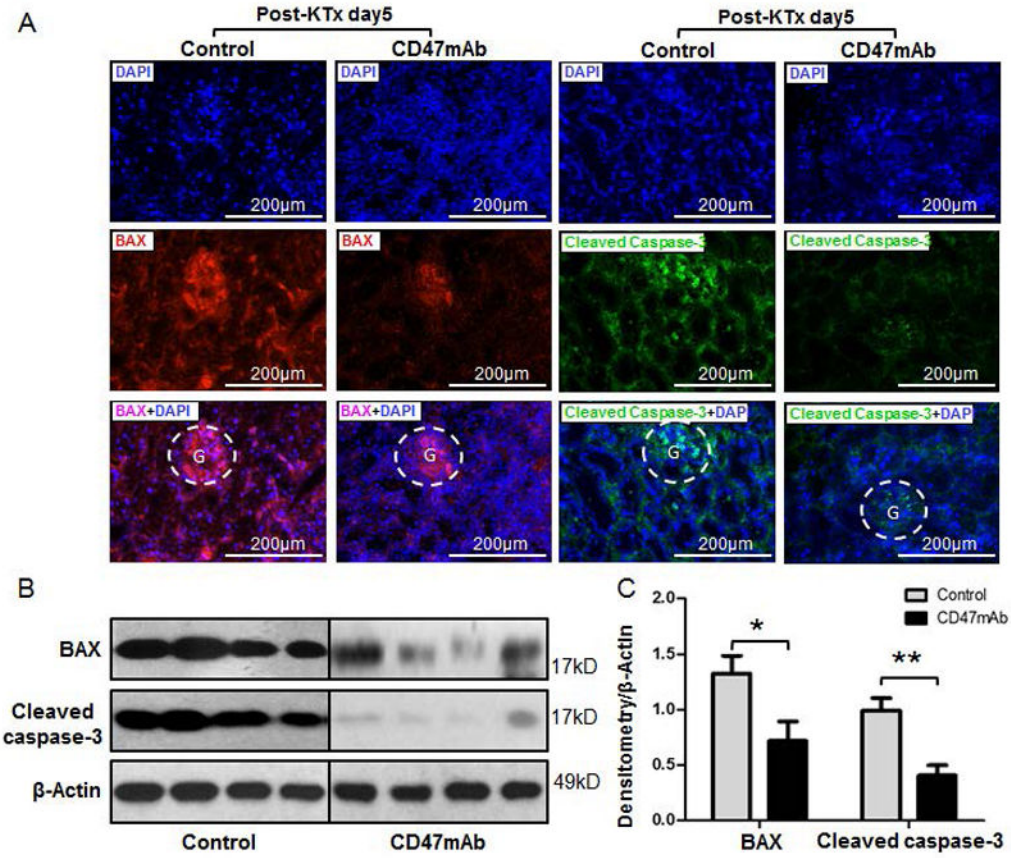

Figure 7. CD47mAb treatment minimized the apoptosis of DCD kidney after transplantation

(A) Immunofluorescence staining showed a decrease of Bcl-2-associated X protein (BAX) and Caspase-3 in the CD47mAb treated renal allografts compared to control. Western blotting (B) and densitometry analysis (C) confirmed the decreasing expression of BAX and Caspase-3 in renal grafts treated with CD47mAb than that in control (n=4/group, *p<0.05 or ** p<0.01, respectively).